

Quantum structures created by nonhomogeneous magnetic fields

F.M. Peeters* and A. Matulis†

Departement Natuurkunde, Universiteit Antwerpen (UIA), Universiteitsplein 1, B-2610 Antwerpen, Belgium

(Received 16 June 1993)

We study a system consisting of magnetic tunneling barriers, in particular we have studied the following structures: magnetic quantum steps, barriers, and magnetic wells. The energy spectrum (bound and scattered states) for these systems is obtained and the nature of the states is discussed.

I. INTRODUCTION

The behavior of electrons in homogeneous magnetic fields has been used extensively to obtain experimental information on properties of charge carriers¹ such as, e.g., their density and the Fermi surface (through the Shubnikov de Haas effect), and their mass (e.g., using cyclotron resonance). Scattering of electrons on magnetic impurities form the other limit in which electrons experience locally (on an angstrom scale) strong magnetic fields which may act as scattering centers in, e.g., diluted semimagnetic materials.²

In the present paper we are interested in the intermediate limit in which electrons interact with magnetic fields which are inhomogeneous on a nanometer scale. There has been recent experimental interest in such systems where it has become possible to create magnetic dots³ and integrate ferromagnetic materials with semiconductors⁴⁻⁶ where patterning of such films was recently demonstrated experimentally.⁷ This new technology will add a new functional dimension to the present semiconductor technology and will open new avenues for new physics and possible applications such as switches based on the Lorentz force and nonvolatile memories based on the Hall voltage generated by a local magnetic field. A different route to create inhomogeneous magnetic fields is through the integration of superconducting materials with semiconductors. This was realized experimentally using type-II superconductors which were deposited on a Si-metal-oxide semiconductor⁸ or a GaAs/AlGaAs heterojunction.^{9,10} Magnetic flux lines penetrate the two-dimensional electron gas (2DEG) which act as nanometer scale scattering centers for the electrons,¹¹⁻¹³ offering the possibility to study weak localization¹⁰ and the dynamics of vortices.¹⁴ Using lithographic techniques, these superconducting films can be patterned into any desired form. The geometry of the patterning determines the geometry of the inhomogeneous magnetic field.

In general the shape anisotropy of the magnetic film (or the stripes) will force the magnetization in the plane of the film. Other mechanisms can be active which can lead to a magnetization vector perpendicular to the film, which is the situation we are interested in. Out-of-plane magnetization has been realized in ultrathin layers of Fe on Ag (Ref. 15) or Cu (Ref. 16) compounds such as MnAlGa,¹⁷ Co/Ni multilayers,¹⁸ ultrathin MnGa

films,⁵ and the metastable MnAl τ phase,⁴ which can be grown epitaxially on GaAs/AlAs heterostructures using molecular-beam epitaxy.

The creation of superlattices by an inhomogeneous magnetic field was proposed theoretically in Refs. 19 and 20. Vil'ms and Éntin²¹ presented a theoretical analysis of the energy spectrum of 2D electrons near domain walls and in a system of parallel magnetic strips. Transport of a 2DEG in the presence of a perpendicular magnetic field modulated weakly and periodically along one direction was studied in Ref. 22. The generalization to 2D magnetic-field modulation is given in Ref. 23. Recently Van Roy, DeBoeck, and Borghs²⁴ studied the geometric factors controlling the magnitude of the demagnetizing field of ferromagnetic thin films with perpendicular magnetization. Different geometries were studied and they found that a grating-type structure with periodicity of a few 100 nm to 1 μ m would give the maximum magnetic-field strength in the underlying semiconductor heterostructure. Müller²⁵ considered a different system in which a 2DEG strip is placed in a perpendicular magnetic field which increases linearly along one direction. He showed that this system has a remarkable time-reversal symmetry.

In the present paper we will consider different configurations of nonuniform magnetic fields in which the nonuniformity is only along one direction and has a typical length scale of the order of nanometers. The electron spectrum of a 2DEG in simple magnetic structures, such as a magnetic step (Sec. III), magnetic barrier (Sec. IV), and magnetic well (Sec. V), is considered and discussed. The similarities and differences between similar potential problems are pointed out.

II. NONHOMOGENEOUS MAGNETIC FIELDS

We consider a 2DEG moving in the (x, y) plane with a magnetic field \mathbf{B} along the z direction. In the single-particle approximation such a system is described by the Hamiltonian

$$H = \frac{1}{2m} \left(\mathbf{p} + \frac{e}{c} \mathbf{A} \right)^2. \quad (2.1)$$

We take the vector potential in the Landau gauge $\mathbf{A} =$

$(0, A, 0)$ and the magnetic field is modulated along the x direction, and thus

$$B_z = B(x) = \frac{d}{dx} A(x). \quad (2.2)$$

Let us introduce the following characteristic parameters: (i) the frequency $\omega_c = eB_0/mc$ with B_0 some typical magnetic field, and (ii) the length $l_B = \sqrt{\hbar c/eB_0}$. From now on we will express all quantities in dimensionless units: (1) the magnetic field $B(x) \rightarrow B_0 B(x)$, (2) the vector potential $A(x) \rightarrow B_0 l_B A(x)$, (3) the time $t \rightarrow t/\omega_c$, (4) the coordinate $\mathbf{r} \rightarrow l_B \mathbf{r}$, (5) the velocity $\mathbf{v} \rightarrow l_B \omega_c \mathbf{v}$, and (6) the energy $E \rightarrow \hbar \omega_c E$.

In these dimensionless units the 2D Schrödinger equation becomes

$$\left\{ \frac{\partial^2}{\partial x^2} + \left(\frac{\partial}{\partial y} + iA(x) \right)^2 + 2E \right\} \Psi(x, y) = 0. \quad (2.3)$$

Because of the special form of the gauge the system is translational invariant along the y direction and as a consequence we can choose the following form for the wave function:

$$\Psi(x, y) = e^{-iqy} \psi(x), \quad (2.4)$$

where $-q = k_y$ is the wave vector of the electron in the y direction. The wave function $\psi(x)$ actually satisfies the following 1D Schrödinger equation:

$$\left\{ \frac{d^2}{dx^2} - [A(x) - q]^2 + 2E \right\} \psi(x) = 0, \quad (2.5)$$

where the function

$$V(x) = \frac{1}{2} [A(x) - q]^2 \quad (2.6)$$

can be interpreted as a q -dependent electrical potential. Note that in the case of 1D magnetic-field modulation studied in the present paper there is an analogy between the magnetic field and the potential given by the following relation:

$$B(x) = \frac{1}{\sqrt{2V(x)}} \frac{dV(x)}{dx}. \quad (2.7)$$

A jump in the magnetic field will result in a discontinuity in the derivative of the potential $V(x)$.

III. MAGNETIC STEP

First, let us consider the most simple shape for a non-homogeneous magnetic field: the magnetic step. In this situation the magnetic field fills the half space $x > 0$, as shown in Fig. 1(a) (solid curve), which is described by

$$B(x) = \theta(x) \quad (3.1)$$

with the corresponding vector potential [dashed curve in Fig. 1(a)]

$$A(x) = x\theta(x), \quad (3.2)$$

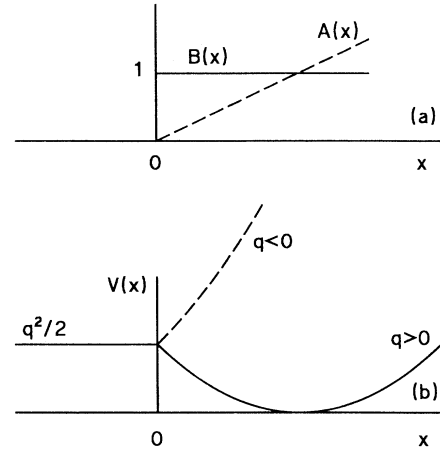


FIG. 1. Magnetic step: (a) the magnetic field $B(x)$ (solid curve) and the vector potential $A(x)$ (dashed line), and (b) the equivalent potential for $q > 0$ (solid curve) and $q < 0$ (dashed curve).

where $\theta(x) = 1(x \geq 0), 0(x < 0)$ is the step function. There are two different cases which we have to consider, and of which the resulting potential is illustrated in Fig. 1(b).

Case 1 ($q > 0$). As seen in Fig. 1(b) (solid curve), the potential $V(x)$ has the form of an asymmetric quantum well which deepens with increasing q . It is well known²⁶ that such a well can have a bound state if the well is sufficiently deep. Thus we have to consider separately (a) $E < q^2/2$, where bound eigenstates are expected to appear in the region $x \sim q$; and (b) $E > q^2/2$, which corresponds to scattered states, describing the electron reflection by the magnetic step. The appearance of bound states makes this system essentially different from the usual potential step problem where only scattered states exist.

Case 2 ($q < 0$). In this case the equivalent potential is a constant $V(x) = q^2/2$ for $x < 0$ and a barrier in the region $x > 0$ [Fig. 1(b), dashed curve], which is unbounded for $x \rightarrow \infty$. In this case there are only scattered states which correspond to electron reflection by the magnetic barrier.

For $x > 0$ the Schrödinger equation takes the form

$$\left\{ \frac{d^2}{dz^2} - \frac{z^2}{4} + p + \frac{1}{2} \right\} \psi(z) = 0, \quad (3.3)$$

with $z = \sqrt{2}(x - q)$ and $p = E - 0.5$. The solutions of it are the Weber functions²⁷ $D_p(z)$, which have the following asymptotic behavior: $D_p(z)|_{z \rightarrow +\infty} \rightarrow 0$. Taking into account (3.2) and comparing Eqs. (3.3) and (2.5) we see that in the region $x > 0$ the wave function becomes

$$\psi(x) \sim D_{E-0.5}[\sqrt{2}(x - q)], \quad (3.4)$$

up to a normalization constant, while for $x < 0$ there is no magnetic field and the wave function is proportional to

$$\psi(x) \sim \exp(x\sqrt{q^2 - 2E}) \quad (3.5)$$

when $E < q^2/2$. Matching the wave functions (3.4) and (3.5) and its first derivative at $x = 0$ we obtain the following equation:

$$\sqrt{q^2 - 2E} = \frac{d}{dx} \ln D_{E-0.5}[\sqrt{2}(x - q)] \Big|_{x=0} \quad (3.6)$$

whose solutions lead to the electron eigenvalues $E = E_n(q)$ with the corresponding wave function $\psi_{nq}(x)$.

Once we know the eigenvalues and the corresponding wave function we can obtain the other characteristics of the bound states. Differentiating Eq. (2.5) by $\partial/\partial q$, multiplying it by the corresponding wave function $\psi_{nq}(x)$, and integrating over x we find

$$\int_{-\infty}^{\infty} dx \psi_{nq}(x) \left\{ 2 \left[A(x) - q + \frac{d}{dq} E_n(q) \right] \psi_{nq}(x) + \left[\frac{d^2}{dx^2} - [A(x) - q]^2 + 2E_n(q) \right] \frac{\partial}{\partial q} \psi_{nq}(x) \right\} = 0. \quad (3.7)$$

The second part of Eq. (3.7) contains the Schrödinger equation and is equal to zero. Finally we obtain the average electron velocity of the bound state along the magnetic step (y direction)

$$-v_n(q) \equiv \int_{-\infty}^{\infty} dx \psi_{nq}^2(x) [q - A(x)] = \frac{d}{dq} E_n(q), \quad (3.8)$$

where the minus sign results from the definition $q = -k_y$. Analogously the mean electron position along the x axis $X_n(q)$ can be obtained. We multiply Eq. (2.5) by $d\psi_{nq}/dx$, integrate over x , and find

$$\int_{-\infty}^{\infty} dx \left(\frac{1}{2} \frac{d}{dx} \frac{d\psi_{nq}(x)}{dx} \right)^2 - \left\{ \frac{1}{2} [(A(x) - q)^2 - 2E_n(q)] \frac{d}{dx} \psi_{nq}^2(x) \right\} = \int_{-\infty}^{\infty} dx \psi_{nq}^2(x) [A(x) - q] \theta(x) = 0, \quad (3.9)$$

which can be reduced to

$$\int_0^{\infty} dx \psi_{nq}^2(x) [A(x) - q] = 0. \quad (3.10)$$

Now taking into account Eqs. (3.8) and (3.10) and the fact that the electron wave function has the simple form (3.5) in the region $x < 0$ we find the simple relation

$$X_n(q) = \int_{-\infty}^{\infty} dx x \psi_{nq}^2(x) = q + \left(1 + \frac{1}{2q\sqrt{q^2 - 2E_n(q)}} \right) v_n(q). \quad (3.11)$$

The numerical results of the solution of Eq. (3.6) are depicted in Fig. 2(a) by the solid curves, for the lowest three eigenvalues. These curves start at a certain q value (denoted by the solid dot in Fig. 2), which is a function of n . The corresponding results for the average electron velocity $v_n(q)$ (solid curves) and mean electron position $X_n(q)$ (dashed curves) are shown in Fig. 2(b). Notice that the eigenvalues asymptotically, i.e., $q \rightarrow \infty$, reach the values $(n + 1/2)$ for Landau levels in a homogeneous magnetic field, as it should be. In this asymptotic limit the mean electron position approaches $X_n(q) \sim q$ and the average electron velocity tends to zero. In this limit the electron is situated far from the magnetic step and is not influenced by the $x < 0$ region. With decreasing q the electron wave function starts to experience the magnetic step: (1) its energy decreases, because part of the wave function will be situated in a region with zero magnetic field where the electron will have a smaller kinetic energy; (2) its average position is less than q , because the wave function is sucked into the $x < 0$ region; and (3) its velocity increases and the electron runs along the step. From Figs. 2(a) and 2(b) we notice that the width of the transition region, i.e., the q region where $E_n < (n + 1/2)$, is narrower with increasing n . The above properties of these bound states forces us to make the analogy with

edge states.²⁸ Nevertheless there are a number of differences: (1) the available q space for edge states increases with increasing Landau level number n , which is opposite to the behavior of the present bound states; (2) the direction of the velocity is opposite as compared to those of the usual edge states; and (3) the magnitude of the velocity satisfies $|v_n(q)| \leq q$, which is different from edge states which do not have an upper bound on their velocity.

From Fig. 2 we notice that there exist critical values q_n^* such that for $q < q_n^*$ no bound states are found. These points are indicated by the dots on Fig. 2(a) and are situated on the free-electron spectrum curve $E = q^2/2$ [dashed curve in Fig. 2(a)]. For the plotted curves we found the critical values $q_0^* = 0.768$, $q_1^* = 1.623$, and $q_2^* = 2.155$ at which the eigenenergy curve $E_n(q)$ is tangent to the $E = q^2/2$ curve. At these points the electron velocity equals the free-electron value $-v_n = q$, and $X_n(q) \rightarrow -\infty$. The electron wave function $\psi_{n,q}(x)$ is shown in Fig. 3 for the $n = 0$ case and different values of the wave vector q . This figure nicely illustrates the increasing leakage of the wave function into the $x < 0$ region with decreasing q value and the concomitant increasing asymmetry of the wave function.

The wave functions corresponding to the scattered

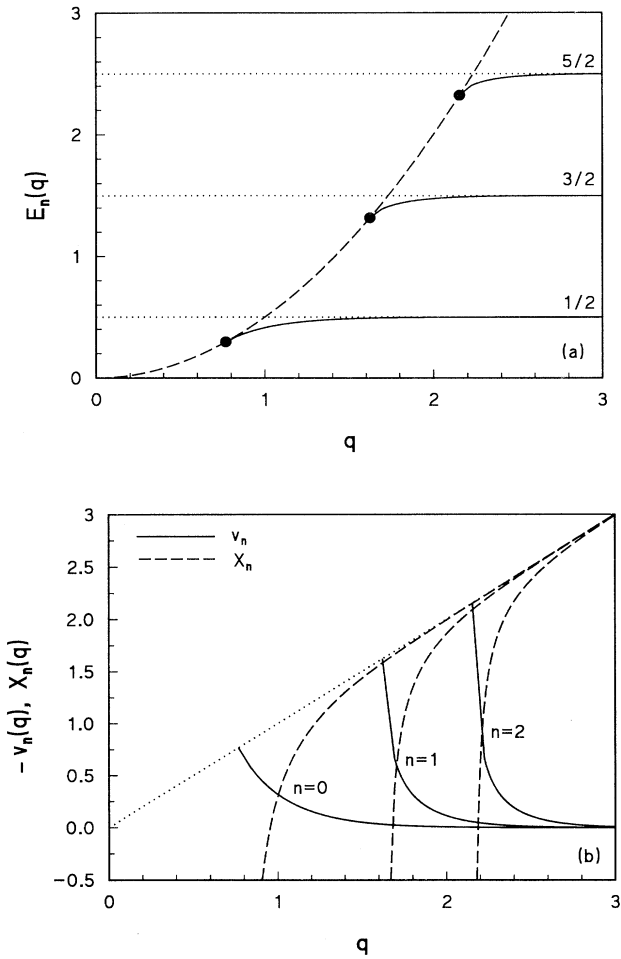


FIG. 2. (a) The energy spectrum for the bound states (solid curves) and (b) the corresponding average velocity along the magnetic step $v_n(q)$ (solid curves) and the electron average position $X_n(q)$ along the x axis (dashed curve) for the magnetic field configuration of Fig. 1.

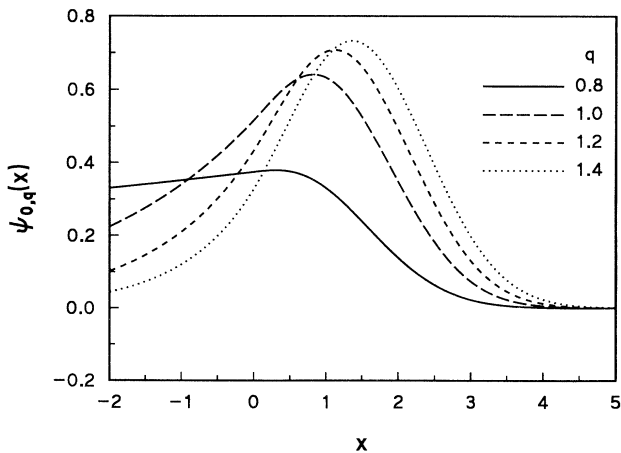


FIG. 3. The electron wave function for the lowest bound state for different values of the electron momentum in the y direction (q) in the case of a magnetic step.

states [case (1): $q > 0$, $E > q^2/2$ and case (2): $q < 0$] can be constructed by matching the function (3.4) valid for $x > 0$ and

$$\psi \sim \sin(\sqrt{2E - q^2}x + \delta), \quad (3.12)$$

valid for $x < 0$ at $x = 0$. This matching has to be done at any electron energy $E > q^2/2$. Examples of those scattered state wave functions are shown in Figs. 4(a) for case (1) and 5(a) for case (2). Notice that the wave functions have a different penetration depth into the magnetic-field region which depends on the sign of q . The physical meaning of the different penetration is clear from the classical electron trajectories in the x, y plane which are shown in Figs. 4(b) and 5(b) for the corresponding q values and which will be discussed in next paragraph.

For comparative purposes we include here the classical analysis of the problem. In the above dimensionless variables the electron trajectory in a magnetic field is given by

$$\begin{aligned} x(t) &= x_0 + \sqrt{2E} \sin(t + \phi), \\ y(t) &= y_0 - \sqrt{2E} \cos(t + \phi), \end{aligned}$$

and the corresponding velocity components are

$$\begin{aligned} v_x(t) &= \sqrt{2E} \cos(t + \phi), \\ v_y(t) &= \sqrt{2E} \sin(t + \phi). \end{aligned}$$

Reflected states originate from the $x < 0$ region and impede ($v_x > 0$) on the magnetic barrier. When the electron penetrates the barrier with velocity $[v_x(0), v_y(0)]$ it performs a circular orbit around the point $(x_0, y_0) = [-v_y(0), v_x(0)]$ and leaves the magnetic step with a velocity $[-v_x(0), v_y(0)]$ after a dwell time $t_d = \pi - 2 \arctan[v_y(0)/v_x(0)]$. The electron is shifted by $2v_x$ in the y direction. Notice that for negative $v_y(0)$ we have $x_0 > 0$ and the dwell time t_d is larger and consequently also the penetration of the electron in the barrier region as is also apparent from Figs. 4(b) and 5(b).

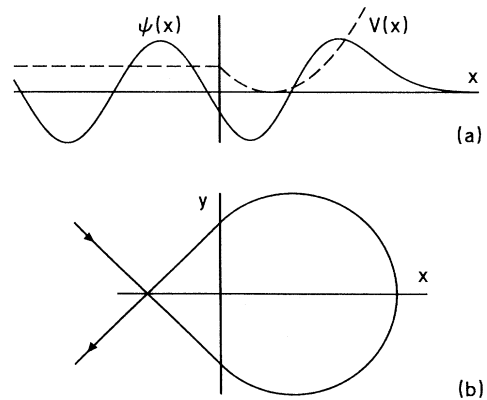
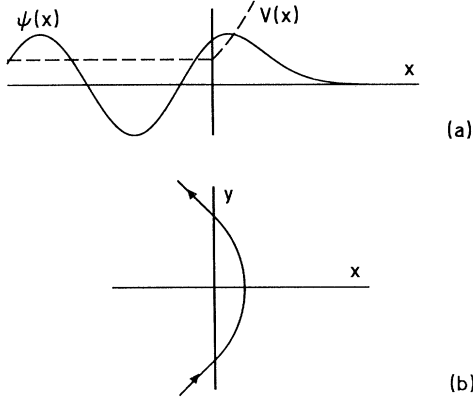


FIG. 4. For $E = 2$ and $q = 1$ we show: (a) the wave function for a scattered state (solid curve) together with the potential $V_q(x)$ (dashed curve), and (b) the classical trajectory of the electron which is reflected by the magnetic step.

FIG. 5. The same as Fig. 4, but now for $E = 2$ and $q = -1$.

In the case of bounded states we formally connect the classical electron energy with the Landau level energy $E = n + 1/2$ and find for the characteristic radius of the electron trajectory $R_c = \sqrt{2n + 1}$. Classically the electron is confined when $x_0 > R_c$ and consequently we obtain for the confinement condition $q = x_0 > \sqrt{2n + 1} = q_n^*$. These classical critical values $q_0^* = 1$, $q_1^* = 1.732$, and $q_2^* = 2.236$ are more restrictive than those obtained from our quantum-mechanical calculation. For large n the classical values for q_n^* approach the quantum-mechanical results.

Notice that in the present magnetic step case the transmission coefficient is always zero. Independent of the strength of the magnetic field and the magnitude of the electron energy, an electron impeding on the magnetic barrier will always be reflected, which is a consequence of the Lorentz force acting on the electron. In this respect this system is different from the textbook potential step problem in which the reflection coefficient becomes different from zero when the electron energy is larger than the potential barrier height.

IV. MAGNETIC BARRIER

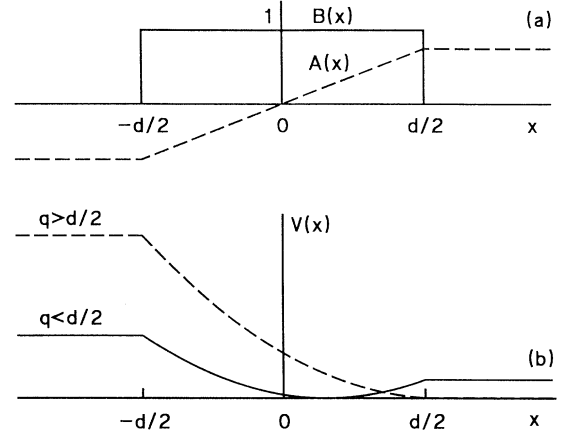
The magnetic step can be used as a building block from which more complicated structures can be built. As a first example we consider the magnetic barrier in which the magnetic field is different from zero in a strip of width d , as shown in Fig. 6(a) by the solid line. In this case the magnetic field has the following form in dimensionless units:

$$B(x) = \theta(d^2/4 - x^2), \quad (4.1)$$

and we choose the vector potential as follows:

$$A(x) = \begin{cases} -d/2, & x < -d/2 \\ x, & |x| \leq d/2 \\ d/2, & x > d/2, \end{cases} \quad (4.2)$$

as is depicted in Fig. 6(a) by the dashed line. The analogous potential $V(x)$ of (2.6) is shown in Fig. 6(b), which depends on the value of the wavevector q : when $|q| < d/2$

FIG. 6. Magnetic barrier: (a) the magnetic field (solid curve) and the vector potential (dashed curve), and (b) the equivalent electric potential $V_q(x)$ for two values of the electron wave vector.

(solid curve) the potential consists of an asymmetric well of finite height, and when $|q| > d/2$ (dashed curve) it is a gradual step. The problem is symmetric under the substitution $q \rightarrow -q$ (and $x \rightarrow -x$) and consequently we may limit ourselves to the case $q \geq 0$.

By inspection of Fig. 6(b) we notice that there are three different energy regions important to us: (1) $0 \leq E \leq (d/2 - q)^2/2$, where bound eigenstates can exist; (2) $(d/2 - q)^2/2 < E \leq (d/2 + q)^2/2$, which is the reflection region; and (3) $(d/2 + q)^2/2 < E$, where the electron is transmitted through the magnetic barrier.

First let us concentrate on the situation in which we have bounded electron states. In this case the electron wave function in the barrier region, i.e., $|x| < d/2$, is a linear combination of Weber functions

$$\psi(x) = aD_{E-0.5}[\sqrt{2}(x - q)] + bD_{E-0.5}[\sqrt{2}(q - x)], \quad (4.3)$$

which we must match (and its first derivative) to the free-electron wave functions of the form (3.5) at the points $x = \pm d/2$. This matching results into the equation

$$F^+(-q + d/2)F^-(q + d/2) - G^+(q - d/2)G^-(-q - d/2) = 0 \quad (4.4)$$

where

$$F^\pm(z) = \sqrt{(q \pm d/2)^2/2 - ED_{E-0.5}(\sqrt{2}z)} + D'_{E-0.5}(\sqrt{2}z) \quad (4.5)$$

and

$$G^\pm(z) = \sqrt{(q \pm d/2)^2/2 - ED_{E-0.5}(\sqrt{2}z)} - D'_{E-0.5}(\sqrt{2}z). \quad (4.6)$$

Equation (4.4) was solved numerically. The results for a wide magnetic barrier ($d = 5$) are shown in Fig. 7 by the

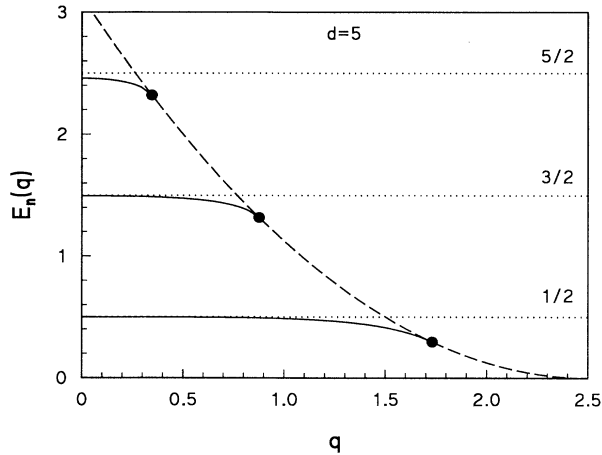


FIG. 7. The energy spectrum for the bound states (solid curves) in a magnetic barrier of width $d = 5$. Dashed curve $E = (d/2 - q)^2/2$ indicates the free-electron spectrum.

solid curves which end at the solid dots. The latter are situated on the $E = (q - d/2)^2/2$ curve (dashed curve). Notice that the spectrum resembles the one of the magnetic step case [see Fig. 2(a)] with the distinction that the latter has an infinite number of branches while the one for a magnetic barrier has a finite number of bound states for each q . For $d = 5$ there are only three branches in the energy spectrum. The number of energy branches decreases with decreasing barrier width d . Irrespective of the value of d there is always *at least one* discrete energy value for $q = 0$. This is a consequence of the fact that for $q = 0$ the potential $V(x)$ is one dimensional and symmetric. Such a potential is known to have at least one discrete eigenvalue²⁶ irrespective of the size of the potential well. The value of the lowest branch in the spectrum is plotted in Fig. 8 for $q = 0$ as a function of the barrier

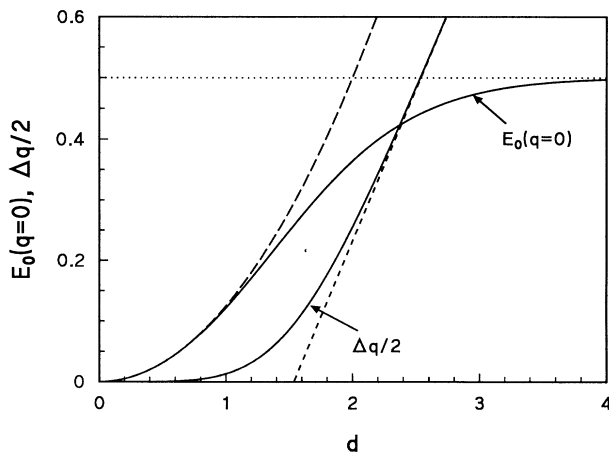


FIG. 8. The lowest eigenvalue of the bound state in a magnetic barrier as function of the barrier width for $q = 0$ and the width (Δq) of the lowest-energy branch in q space (solid curves). The long-dashed curve indicates the height of the potential $V_{q=0}(x = d/2) = d^2/8$ and the short-dashed line $\Delta q/2 = d/2 - q_0^*$ indicates the asymptotic value of that width defined from the magnetic step spectrum.

width d . Notice that when $d < 1$ (i.e., when the magnetic barrier width is less than the magnetic length l_B) the eigenvalue approaches $E_0(q = 0) \approx (d/2)^2/2$, which is shown by the long-dashed curve in Fig. 8. Although the electron is bound to the barrier, in the case of small- d values the electron wave function is situated mainly outside the barrier and consequently its energy approaches the height of the potential well $V(d/2)$. The width in q space (Δq) of the lowest-energy branch is also given in Fig. 8. It is seen that this width decreases rapidly to zero when $d < 1$ and in the opposite case (when $d \rightarrow \infty$) it asymptotically reaches the line $\Delta q/2 = d/2 - q_0^*$ (short-dashed line), where $q_0^* = 0.768$ is the value as obtained from the magnetic step spectrum. Another distinction as compared to the magnetic barrier spectrum [see Fig. 2(a)] is that the energy eigenvalues are smaller in magnitude than those in the magnetic step case.

For the unbounded states we have calculated the transmission coefficient which now depends not only on the electron energy but also on the electron wave vector q in the y direction. In the present case tunneling is a two-dimensional process in which the total electron wave vector and the electron energy is conserved but the direction of the wave vector is altered. A contour plot of the transmission coefficient $T(q, E)$ versus initial electron velocity components (v_x, v_y) is shown in Fig. 9 for a magnetic barrier of width $d = 5$. The quantum transition coefficient is zero above the line $v_y = (v_x^2 - d^2)/2d$, which is the result one would obtain from classical mechanics and which defines a semi-infinite transmission window. Below this line we have classically $T = 1$, but quantum mechanically $T(q, E)$ gradually increases with increasing electron energy. For rather thick barriers (as in the case of $d = 5$) there is some additional structure at low energy which is enlarged in the inset of Fig. 9. There is an additional peak around $(v_x, v_y) = (0.3, -2.5)$, which

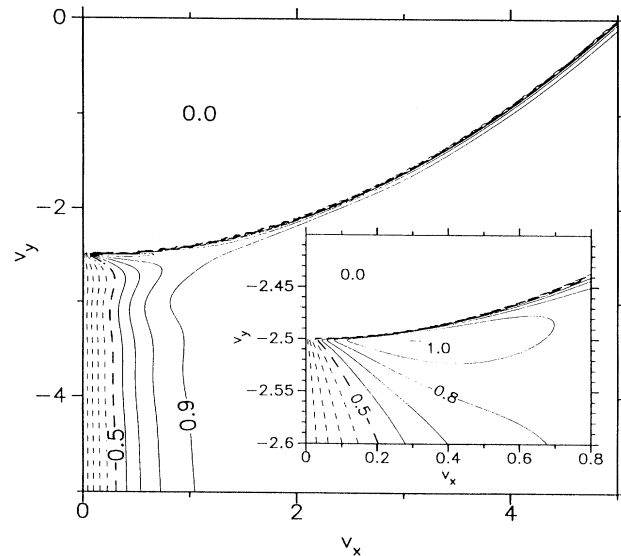


FIG. 9. Contour plot of the transmission coefficient through a magnetic barrier in the incident electron velocity (v_x, v_y) space.

is a consequence of the presence of a virtual energy level above the quantum well $V_q(x)$.

V. MAGNETIC WELL

The inverse situation of the previous problem is the magnetic well case, which we will discuss now. Because of the essential 2D character of the electron motion in a magnetic field we should rather speak of a magnetic wire. In dimensionless units the magnetic field is given by

$$B(x) = \begin{cases} 0, & |x| \leq d/2 \\ 1, & |x| > d/2 \end{cases} \quad (5.1)$$

and the corresponding vector potential is

$$\begin{aligned} & \left[\cos(kd)D_{E-0.5}(\sqrt{2}q) - \frac{\sqrt{2}}{k} \sin(kd)D'_{E-0.5}(\sqrt{2}q) \right] D'_{E-0.5}(-\sqrt{2}q) \\ & + \left[\cos(kd)D'_{E-0.5}(\sqrt{2}q) + \frac{k}{\sqrt{2}} \sin(kd)D_{E-0.5}(\sqrt{2}q) \right] D_{E-0.5}(-\sqrt{2}q) = 0 \end{aligned} \quad (5.4)$$

where $k = \sqrt{2E - q^2}$ for $2E > q^2$ and $k = i\sqrt{q^2 - 2E}$ for $2E < q^2$ in which case the trigonometric functions should be replaced by their corresponding hyperbolic functions.

The results of the numerical solution of this equation are presented in Fig. 10(a) for a wide well (i.e., $d = 5$) and in Fig. 10(b) for a narrow well (i.e., $d = 1$). In the wide well case [Fig. 10(a)] there are clearly two distinct regions which are separated by the free-electron energy $E = q^2/2$ curve [dashed curve in Fig. 10(a)]. For $E \ll q^2/2$ the energy spectrum consists of Landau levels. The electron is mainly located in the barrier where there exists a uniform magnetic field. For small- q values, i.e., $E \gg q^2/2$, the spectrum consists of bands with free-electron-like motion in the y direction. This is similar to the case of the well-known quantum wire with electrical potential barriers. When we decrease the width of the well the two regions are less distinct, as is apparent in Fig. 10(b) for the case of $d = 1$. For $d = 1$ the well is narrower than the width of the electron wave function and consequently there is always an appreciable overlap of the wave function with the magnetic barrier region. Notice that the energy levels have almost no dispersion. The different behavior between the two cases is also illustrated in Fig. 11 where the electron velocity is shown for the different states. Notice that the velocity exhibits a maximum near $E = q^2/2$ and it diminishes quickly for $q \gg \sqrt{2E}$, which is the region where the electron is mainly located inside the magnetic barrier. Notice that for wide wells, i.e., see the $d = 5$ case, the velocity curve $v_n(q)$ can have several local maxima, which is a consequence of the repulsion of the different energy levels as seen in Fig. 10(a). In the case of the usual quantum wire constructed from walls consisting of potential barriers the electron velocity is $v_n = \hbar k_y = -q$ and it is independent of the energy-level index n and it is a uniformly increasing function of the

$$A(x) = \begin{cases} x - d/2, & x > d/2 \\ 0, & |x| \leq d/2 \\ x + d/2, & x < -d/2. \end{cases} \quad (5.2)$$

The value of the vector potential is now unbounded, i.e., $A(x)|_{x \rightarrow \pm\infty} \rightarrow \pm\infty$, and as a consequence the potential satisfies $V(x)|_{x \rightarrow \pm\infty} \rightarrow \infty$, which implies that the electron motion is confined in the x direction and all the states are bounded.

The corresponding wave functions are constructed by matching the quasi-free-electron wave function (3.12) in the region $|x| < d/2$ with the Weber functions

$$\psi(x) = D_{E-0.5}[\pm\sqrt{2}(x \mp d/2 - q)], \quad (5.3)$$

which are valid in the regions $|x| > d/2$. This matching of the wave function and its first derivative leads to the following algebraic equation for the eigenvalues:

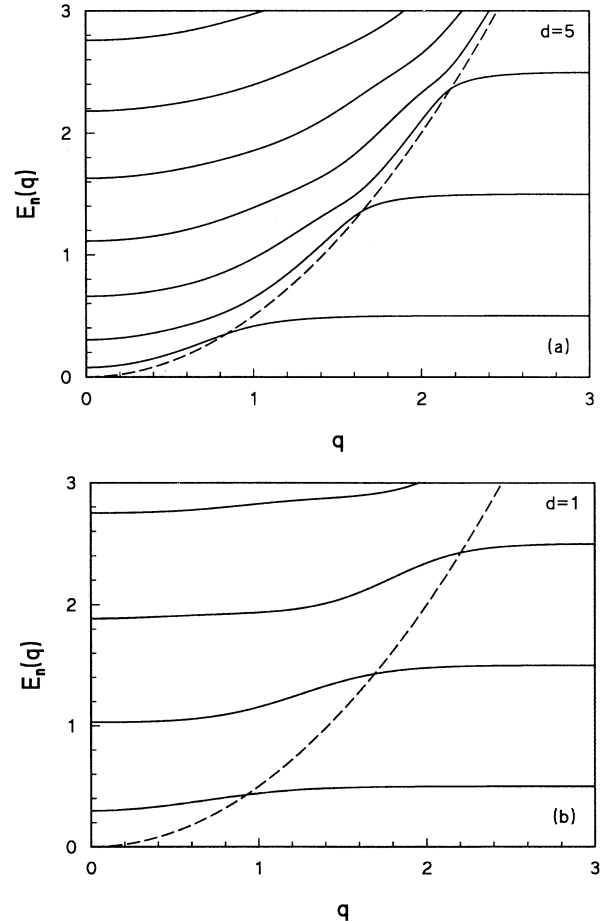


FIG. 10. The energy spectrum of a magnetic well for two different values of the width: (a) $d = 5$ and (b) $d = 1$.

electron wave vector. The behavior of $v_n(q)$ as depicted in Fig. 11 is also different from the one of edge states in which $v_n(q)$ is a uniform increasing function of q .

The density of states (DOS) for the two cases is depicted in Fig. 12. Notice that, like for the quantum wire case, the DOS exhibits singularities at the onset of each energy level. But there is a difference: the width in energy space of each level is finite and bounded by a singularity in the DOS. Suppose we have a system in which we are able to increase the Fermi energy gradually. Starting from zero, we first populate the quantum wire states and the electrons are mainly situated in the well region. Further increasing the Fermi energy we see that for $d = 5$ we first start to populate the next energy level, which consists initially of states located inside the well. For $d = 1$, on the other hand, we start to populate states which are situated in the magnetic barrier region and which are nothing other than 2D Landau states. Thus by changing the Fermi level we are able to have 1D states or 2D states at the Fermi level, which will have considerable influence on the electrical properties of the system. The 1D states are quasifree while the 2D states are localized on Landau orbits and can only move if scattering is involved.

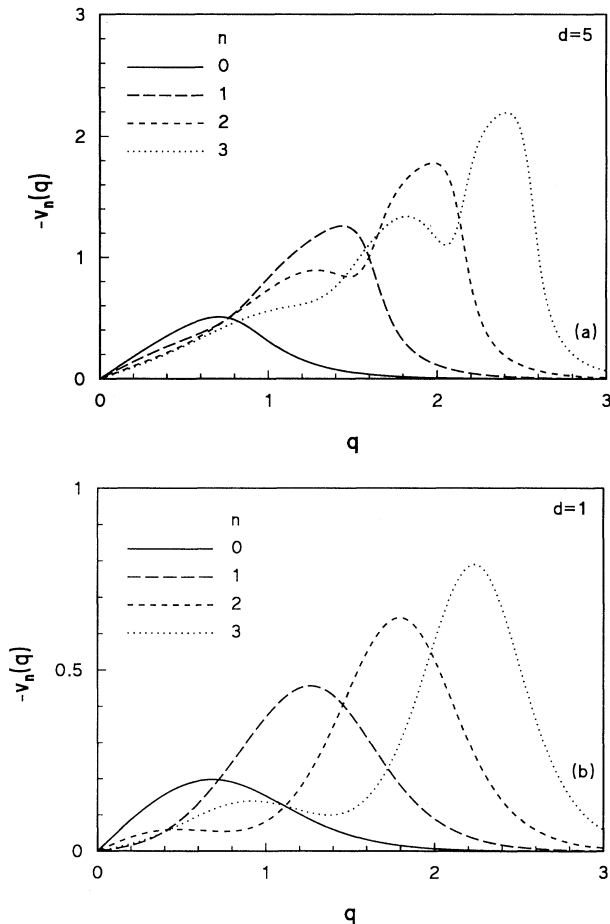


FIG. 11. The electron average velocity corresponding to the energy spectrum of Fig. 10.

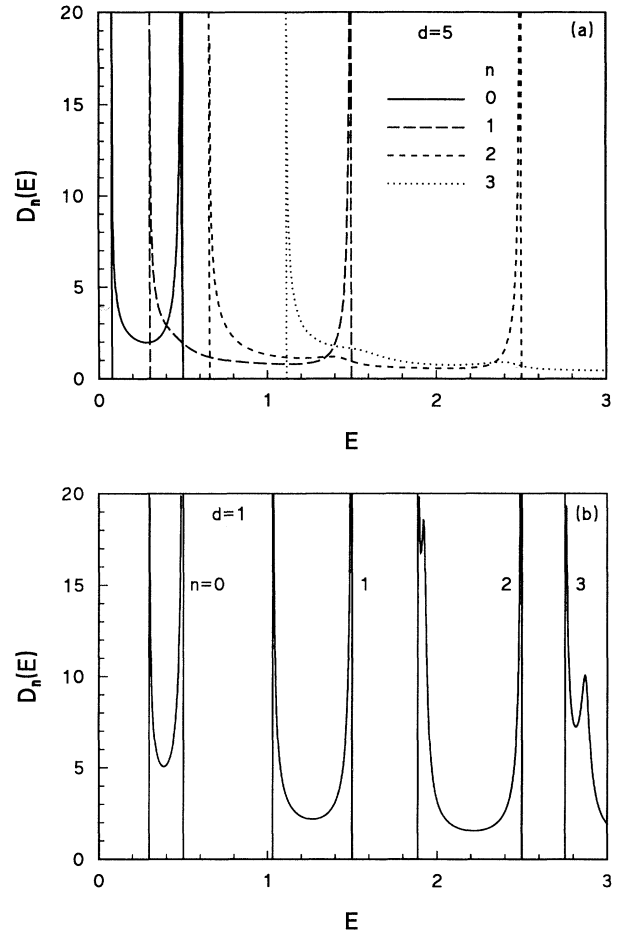


FIG. 12. The density of states of the electron states in the magnetic wells corresponding to Fig. 10.

VI. CONCLUSION

The spectrum of electrons moving in 2D and interacting with nonhomogeneous magnetic fields is calculated. Different structures of nonhomogeneous magnetic fields in one direction are considered. The similarities and differences between similar structures built from electrical potentials are pointed out. The motion in the present case is essential 2D while in the electrical potential problems often a separation of variables is possible, which reduces the problem to 1D. In the present case the problem can mathematically be cast into a 1D problem, but the physics and the motion stay essentially 2D. In the magnetic case the potential $V_q(x)$ appearing in the mathematical 1D problem depends on the electron wave vector (q), which makes it inherently two dimensional even in the case of one-dimensional magnetic-field modulations.

One of the interesting features of nonhomogeneous magnetic-field structures is that a step in the magnetic field can bind electrons. This is essentially different from potential steps, which always act repulsive. As a consequence magnetic barriers can exhibit bound states and tunneling through them turns out to be much more rich:

for example, tunneling can occur through such bound states which may lead to quiresonances in the transmission coefficient. Tunneling is essentially a 2D process where only transmission is possible in a semi-infinite window in velocity space. Such a magnetic barrier structure can be used as a filter for electron wave vectors. A combination of such magnetic barriers will result in more complicated structures such as, for example, resonant tunneling structures and superlattices, which will be studied in a forthcoming paper.²⁹

The inhomogeneous magnetic fields discussed in the present paper can be created by depositing a type-I superconducting film above a 2DEG and using patterning techniques to create the desired magnetic-field profile in the 2DEG. The use of ferromagnetic films will in gen-

eral lead to more complicated magnetic-field profiles, the theoretical study of which is in progress. In the present paper we have limited ourselves to the most simple structures from which the basic physics is already apparent.

ACKNOWLEDGMENTS

This work is supported by the Belgian National Science Foundation (NFWO) and by the Interuniversity Microelectronics Center (IMEC, Leuven). One of us (A.M.) acknowledges the support of the EEC through the program "Cooperation in Science and Technology with Central and Eastern European Countries." One of us (F.M.P.) acknowledges fruitful discussion with P. Vasilopoulos.

* Electronic address: peeters@nats.uia.ac.be

† Permanent address: Semiconductor Physics Institute, Gostauto 11, 2600 Vilnius, Lithuania.

¹ D. Shoenberg, *Magnetic Oscillations in Metals* (Cambridge University Press, Cambridge, 1984).

² For a review see, e.g., J.K. Furdyna, *J. Appl. Phys.* **64**, R29 (1988).

³ M.A. McCord and D.D. Awschalom, *Appl. Phys. Lett.* **57**, 2153 (1990).

⁴ T. Sands, J.P. Harbison, M.L. Leadbeater, S.J. Allen, Jr., G.W. Hull, R. Ramesh, and V.G. Keramidas, *Appl. Phys. Lett.* **57**, 2609 (1990); M.L. Leadbeater, S.J. Allen, Jr., F. DeRosa, J.P. Harbison, T. Sands, R. Ramesh, L.T. Florez, and V.G. Keramidas, *J. Appl. Phys.* **69**, 4689 (1991); T. Sands, J.P. Harbison, S.J. Allen, Jr., M.L. Leadbeater, T.L. Cheeks, M.J.S.P. Brasil, C.C. Chang, R. Ramesh, L.T. Florez, F. DeRosa, and V.G. Keramidas, in *Magnetic Thin Films, Multilayers and Surfaces*, edited by S. S. P. Parkin, MRS Symposia Proceedings No. 231 (Materials Research Society, Pittsburgh, 1992), p. 341.

⁵ M. Tanaka, J.P. Harbison, J. DeBoeck, T. Sands, B. Philips, T.L. Cheeks, and V.G. Keramidas, *Appl. Phys. Lett.* **62**, 1565 (1993).

⁶ K.M. Krishnan, *Appl. Phys. Lett.* **61**, 2365 (1992).

⁷ W. Van Roy, E.L. Carpi, M. Van Hove, A. Van Esch, R. Bogaerts, J. De Boeck, and G. Borghs, *J. Magn. Mater.* **121**, 197 (1993).

⁸ G.H. Kruithof and T.M. Klapwijk, in *Proceedings of the 19th International Conference on the Physics of Semiconductors, Warsaw 1988*, edited by W. Zawadzki (Polish Academy of Sciences, Warsaw, 1989), p. 499.

⁹ A.K. Geim, *Pis'ma Zh. Eksp. Teor. Fiz.* **50**, 359 (1989) [*JETP Lett.* **50**, 389 (1990)]; A.K. Heym, S.V. Dubonos, and A.V. Khaetskii, *ibid.* **51**, 107 (1990) [*ibid.* **51**, 121 (1990)].

¹⁰ S.J. Bending, K. von Klitzing, and K. Ploog, *Phys. Rev. Lett.* **65**, 1060 (1990).

¹¹ J. Rammer and A.L. Shelankov, *Phys. Rev. B* **36**, 3135 (1987).

¹² A.V. Khaetskii, *J. Phys. C* **3**, 5115 (1991).

¹³ L. Brey and H.A. Fertig, *Phys. Rev. B* **47**, 15961 (1993).

¹⁴ G.H. Kruithof, P.C. van Son, and T.M. Klapwijk, *Phys. Rev. Lett.* **67**, 2725 (1991).

¹⁵ B.T. Jonker, K.H. Walker, E. Kisher, G.A. Prinz, and C. Carbone, *Phys. Rev. Lett.* **57**, 142 (1986).

¹⁶ C. Liu, E.R. Moog, and S.D. Bader, *Phys. Rev. Lett.* **60**, 2422 (1988).

¹⁷ R.C. Sherwood, E.A. Nesbitt, J.H. Wernick, D.D. Bacon, A.J. Kurtzig, and R. Wolfe, *J. Appl. Phys.* **42**, 1704 (1971).

¹⁸ G.H.O. Daalderop, P.J. Kelly, and F.J.A. den Broeder, *Phys. Rev. Lett.* **68**, 682 (1992).

¹⁹ B.A. Dubrovin and S.P. Novikov, *Zh. Eksp. Teor. Fiz.* **79**, 1006 (1980) [*Sov. Phys.—JETP* **52**, 511 (1980)].

²⁰ D. Yoshioka and Y. Iye, *J. Phys. Soc. Jpn.* **56**, 448 (1987).

²¹ P.P. Vil'ns and M.V. Éntin, *Fiz. Tekh. Poluprovodn.* **22**, 1905 (1988) [*Sov. Phys.—Semicond.* **22**, 1209 (1988)].

²² P. Vasilopoulos and F.M. Peeters, *Superlatt. Microstruct.* **4**, 393 (1990); F.M. Peeters and P. Vasilopoulos, *Phys. Rev. B* **47**, 1466 (1993).

²³ X.-G. Wu and S.E. Ulloa, *Phys. Rev. B* **47**, 7182 (1993).

²⁴ W. Van Roy, J. De Boeck, and G. Borghs, *Appl. Phys. Lett.* **61**, 3056 (1992).

²⁵ J.E. Müller, *Phys. Rev. Lett.* **68**, 385 (1992).

²⁶ L.D. Landau and E. Lifshitz, *Quantum Mechanics* (Pergamon Press, Oxford, 1977), p.66.

²⁷ *Handbuch of Mathematical Functions*, edited by M. Abramowitz and I. Stegun (Dover Publications, Inc., New York, 1972), p. 687.

²⁸ J. Hajdu, in *Physics of the Two-Dimensional Electron Gas*, edited by J.T. Devreese and F.M. Peeters (Plenum, New York, 1987), p. 27.

²⁹ A. Matulis, F.M. Peeters, and P. Vasilopoulos (unpublished).